Can. J. Remote Sensing, Vol. 35, Suppl. 1, pp. S1–S11, 2009

The utility of potential field enhancements for remote predictive mapping

M. Pilkington and P.B. Keating

Abstract. Potential field (gravity and magnetic) data are fundamental to geologic mapping approaches based on geophysical interpretations. Lithologic and structural information can be extracted from amplitudes and trends of the gravity and magnetic anomalies. To assist in the interpretation, data enhancements are commonly used to transform the original data into new quantities that emphasize or suppress some specified component, resulting in a more easily interpreted representation. The number of available enhancements is rapidly increasing and begs the following question: Are they all useful and effective? Based on modelling, theoretical arguments, and real data examples, we evaluate 12 enhancements in terms of their effectiveness. Four of the 12 are found to be redundant, giving almost identical results when used for quantitatively mapping the edges of magnetic sources or, equivalently, geologic contacts. Two others produce similar levels of detail, so both enhancements are not needed. Two other enhancements are susceptible to noise in the data, leading to a lack of continuity in the mapped contact locations. One of the enhancements produces extra, false contact locations, which can complicate mapping, especially in areas of complex source distributions. When enhancements are used to derive images for qualitative interpretation, only two out of the four that are appropriate for this kind of interpretation give useful information.

Résumé. Les données de champs de potentiel (gravimétrie et magnétisme) sont des éléments importants des approches à la cartographie géologique basée sur l'interprétation de données géophysiques. Des informations géologiques et structurales peuvent être extraites de l'amplitude et des orientations des anomalies gravimétriques et magnétiques. Afin d'aider l'interprétation, des rehaussements de données sont couramment utilisés, ceux-ci transforment les données originales en de nouvelles variables qui mettent l'emphase, ou suppriment certaines composantes spécifiques, ce qui résulte en une représentation plus facile à interpréter. Le nombre de rehaussements développés augmente rapidement ce qui soulève la question : sont-ils utiles et efficaces? En se basant sur la modélisation, des arguments théoriques, et des exemples de données réelles nous évaluons douze types de rehaussements en fonction de leur efficacité. Quatre des douze sont redondants, donnant des résultats presque identiques lorque utilisés de façon qualitative pour localiser les contacts des sources magnétiques, ou de manière équivalente, des contacts géologiques. Deux autres fournissent des niveaux similaires de détails si bien que ces deux types ne sont pas nécessaires. Deux autres types sont sensibles au bruit dans les données, ce qui entraine une perte dans la continuité de la localisation des contacts cartographiés. Un des rehaussements produit des contacts superflus et faux qui peuvent compliquer la cartographie, particulièrement dans les régions où la distribution des sources est complexes. Lorsque les rehaussements sont utilisés pour produire des images pour une cartographie qualitative, seule deux de ceux qui sont potentiellement utiles fournissent de l'information indépendante.

Introduction

Gravity and magnetic data have long formed the foundation of geologic mapping based on geophysical interpretations (Boyd, 1967) and continue to provide valuable lithologic and structural information at a variety of scales, ranging from small exploration claims to tectonic provinces. In many cases, examination of gravity and magnetic anomalies provides the most efficient and cost-effective means to accurately map geologic features in the third dimension (depth). Contrary to some other remotely sensed data, magnetic measurements are not generally affected by surficial cover materials such as water, ice, sand, soil, clay, and vegetation, which can all be considered nonmagnetic, although exceptions do exist (Gay and Hawley, 1991). On the other hand, gravity data may be affected if the covering layer is thick enough to produce a measurable gravity effect, but in many cases a simple correction for water depth, ice thickness, etc. can be applied to recover the desired geological signal. Like most other remotely sensed data, gravity and magnetic data have continuous spatial coverage and are often freely available as a result of government-sponsored mapping campaigns that commonly cover large percentages of countries.

In terms of information content, magnetic field data provide a mapping of magnetic mineral (predominantly magnetite) concentrations, whereas gravity field data reflect bulk rock

Received 10 March 2009. Accepted 12 July 2009.
Published on the Web at http://pubservices.nrc-cnrc.ca/rp-ps/journalDetail.jsp?jcode=cjrs&=eng on 5 March 2010.

M. Pilkington[1] and P.B. Keating. Geological Survey of Canada, Natural Resources Canada, 615 Booth Street, Ottawa, ON K1A 0E9, Canada.

[1]Corresponding author (e-mail: mpilking@nrcan.gc.ca).

density variations. Since lithologic classification is based primarily on the silicate and not the accessory mineral composition of a rock, magnetic data are not an accurate predictive tool for mapping rock type. In contrast, gravity data are, since density is a function of the constituent mineral content (and their individual densities) of a rock. The magnetization of a rock is the vector sum of the induced (measured by the susceptibility) and remanent magnetization present. The magnetization magnitude may vary over many decades, thus producing a large variation in the corresponding magnetic field strength. Hence, the range of responses from different rock types (and their magnetite distribution) is great. This means magnetic data have a high sensitivity to the underlying magnetic source distribution. In contrast, densities do not vary as widely as magnetizations: less than one decade in terms of grams per cubic centimetre. More specifically, 2–4 g/cm^3 will cover almost all rock types, so the physical property range relevant to gravity data is quite small, but this limited range also means that within a given rock type the variation is also small, and hence more diagnostic.

Gravity data have some advantage as a prediction tool for lithologies; in practice, however, magnetic data are the primary data type used for predictive geological mapping. The main reason is the difference in survey resolution: magnetic data are usually collected at a much closer measurement spacing than gravity data, e.g., regional coverage for magnetics is commonly at a line spacing of 800 m (leading to gridded data at 200 m), whereas regional gravity measurements are often collected at 10–15 km intervals, giving grid spacings down to 2–3 km. These figures are typical of survey parameters used in Canada. This difference has historically been driven by cost levels for the two data types, specifically the requirement that gravity data are collected on the ground (slowly and with possible access problems) compared to rapid airborne acquisition of magnetic data. This situation is changing: airborne gravity surveys are now established and reliable and will likely become more important as cost levels decrease. Currently, in Canada, line-kilometre costs are still 2–10 times higher for gravity data. Typical resolution is about 4 km at a line spacing of 2 km and about 2 km at a line spacing of 500 m. The large difference in resolution or detail between magnetic and gravity datasets means that smaller scale and more subtle features can be detected with the former. Furthermore, even if lithology is not immediately apparent, the shape, texture, and distribution of magnetic anomalies (regardless of their relation to specific lithologies) effectively delineate important structural features such as faults, folds, and styles of deformation. In the following, the discussion focuses on magnetic data, even though all the enhancements discussed can be similarly applied to gravity data.

Predictive geological mapping

The methodology behind geological mapping with magnetic data has not changed greatly over the last 50 years. The approach consists of four main stages, namely classify, calibrate, predict, and revise. The goal is a geological map/interpretation that is a combination of magnetic and geological observations, in which the geology supports the inferences from the magnetic data and the magnetic map confirms and is consistent with the geological observations (Boyd, 1967; Isles et al., 1989; Jacques et al., 1997; Milligan and Gunn, 1997). The classification stage divides the area into subregions, each having similar magnetic character as defined by anomaly texture, trend, and amplitudes. Calibration relates each subregion to the corresponding geology, if known, using any pertinent rock property information available. The prediction stage extrapolates the subregion–geology relationship into unmapped areas. This is where the continuity of the magnetic data becomes crucial in tying together discrete and possibly disparate geological observations. The final stage involves revision: checking the match between the two datasets and then iterating through the whole process to solidify the relationship between magnetics and geology. Within this methodology are two processing streams, one being qualitative, i.e., pattern recognition done by the interpreter (dividing an image or series of images based on the geophysical data into subregions with similar characteristics), and the other being quantitative, i.e., calculating source edge locations to map (inferred) geologic contacts. Previous quantitative approaches used synthetic geological models appropriate to the mapping area to find anomaly shapes caused by specific bodies. A particular characteristic of the calculated anomaly would then be used to assign a body edge position. This was also a way for quick estimates of dip. The general rule that edges are near to inflection points of anomalies could also be applied. Current practices still use the old approach, but now there are many new tools with which to improve its effectiveness. Some of the tools have a quantitative component in that they can be used automatically to map source edge (geologic/magnetic contact) locations and get quantitative estimates of relevant source parameters such as susceptibility and dip.

The new "tools" that we discuss here are enhancements of the data which transform the original data into a new quantity that emphasizes or suppresses some specified component, resulting in a more useful representation, one that is more easily interpreted. Perhaps the earliest enhancements routinely used for gravity and magnetic data were vertical derivatives, which suppress longer wavelength field components likely to be caused by large, deep structures, and emphasize shorter wavelength features, namely those caused by near-surface structures/lithology. Recent developments are not just simple linear transformations of the magnetic data (see Roy and Aina, 1986, who "virtually exhaust all non-trivial possibilities in magnetic transformation"). Now, there are various nonlinear functions of the magnetic field, of which some are independent of field/magnetization direction, some are independent of amplitude, and some are connected directly to geophysical models, e.g., body edges. The vast increase in the number of enhancements available to the interpreter of gravity and magnetic data parallels a similar proliferation of seismic "attributes" used in seismic data interpretation. Chopra and

Marfurt (2007) define attribute as any measure of seismic data that helps us visually enhance or quantify features of interpretation interest. Li (2008) points out the similarities and in some cases equivalences between some gravity and magnetic enhancements and seismic attributes. With numerous attributes available for interpretive work, the question of whether some are redundant, useless, or confusing has been raised (Barnes, 2007). Equally important is the question of not "what do they mean" but "why and how is the attribute related to the physical property of interest?" (Hart, 2008).

We address both of these questions, originally posed for the seismic community, for the growing number of enhancements of potential field data now available for geologic mapping applications. By analyzing the responses of several enhancement techniques on synthetic models we measure their efficacy in locating geologic source positions and specifically their edges. The utility of the techniques are further rated in terms of their robustness in the presence of noise, interference, non-induced magnetizations, and nonvertical structural dips. Aeromagnetic data from the Abitibi Greenstone Belt are used to support the comparison.

Enhancements of potential field data

The enhancements considered here are listed in **Table 1** along with the expressions used for their calculation. We consider only these 12, acknowledging that others do exist, mostly in the form of higher order versions of some of the quantities listed; they are discussed briefly in the following. First, the quantitative processing of magnetic data to extract the locations of geologic contacts is considered. This kind of procedure makes the assumption that the magnetic source or body edges, i.e., where magnetic properties change, correspond to changes in lithology. The locations of these "contacts" are found from characteristics of the given enhanced data. Some enhancements exhibit a maximum value over magnetization contrasts, whereas others change from negative to positive, and so the position of the zero value indicates the contact. Locating maxima is done using the algorithm of Blakely and Simpson (1986). To gauge the utility of these enhancements for such mapping, we use a synthetic model consisting of several bodies and then apply the enhancements to the resulting synthetic magnetic field. **Figure 1** shows a plan view of the model, its field, and the calculated contact locations taken from either the maxima of the enhanced data or the position of the zero contour. The bodies contain no remanent magnetization, and the ambient field is vertical. The rationale for using a vertical field is that even if some transformations are almost nonsensitive to field inclination (analytic signal, AS; local wavenumber, LW; magnitude transform, MT) and remanence direction, most are affected. Therefore, we assume in the case of real data, reduction to the pole is carried out before further processing. This transformation is stable at middle and high geomagnetic latitudes. Two of the 12 enhancements listed in **Table 1** (derivative ratio, DR; directional tilt, Tx) do not have a simple, direct relation to source locations and are not used in this part of the study. Of the other 10, two (vertical gradient, VG; tilt, TI) use the position of the zero value, or contour, to

Table 1. Enhancement methods considered in this study.

Method	Formula	Quantity related to source	Magnitude and dip effects	Reference
Vertical gradient, VG	df/dz	Zero	Yes	Hood, 1965
Derivative ratio, DR[a]	$\tan^{-1}[(df/dx)(\lvert df/dy\rvert^n)]$	—	—	Cooper and Cowan, 2007
Pseudogravity horizontal gradient magnitude, PSG-hgm	$[(dPSG/dx)^2 + (dPSG/dy)^2]^{1/2}$	Max.	Yes	Cordell and Grauch, 1985
Total field horizontal gradient magnitude, TF-hgm	$[(df/dx)^2 + (df/dy)^2]^{1/2}$	Max.	Yes	Grauch et al., 2001
Balanced horizontal gradient magnitude, TDX	$\tan^{-1}\{[(df/dx)^2 + (df/dy)^2]^{1/2}/\lvert df/dz\rvert\}$	Max.	Yes	Cooper and Cowan, 2006
Analytic signal, AS	$[(df/dx)^2 + (df/dy)^2 + (df/dz)^2]^{1/2}$	Max.	No	Roest et al., 1992
Tilt, TI	$\tan^{-1}\{(df/dz)/[(df/dx)^2 + (df/dy)^2]^{1/2}\}$	Zero	Yes	Miller and Singh, 1994
Theta map, TH	$[(df/dx)^2 + (df/dy)^2]^{1/2}/AS$	Max.	Yes	Wijns et al., 2005
Directional tilt, Ty[b]	$\tan^{-1}\{(df/dy)/[(df/dz)^2 + (df/dx)^2]^{1/2}\}$	—	—	Cooper and Cowan, 2006
Tilt horizontal gradient magnitude, THDR	$[(dTI/dx)^2 + (dTI/dy)^2]^{1/2}$	Max.	No	Verduzco et al., 2004
Local wavenumber, LW	$[d^2f/(dxdz)\cdot df/dx + d^2f/(dydz) \times df/dy + d^2f/dz^2\cdot df/dz]/AS^2$	Max.	No	Thurston and Smith, 1997
Magnitude transform, MT[c]	$[X^2 + Y^2 + Z^2]^{1/2}$	Max.	No	Stavrev and Gerovska, 2000

[a]Examples use $n = 1$, where n is the derivative order.

[b]Tx is given by interchanging the x and y terms.

[c]X, Y, and Z are the x, y, and z components, respectively, of the field f.

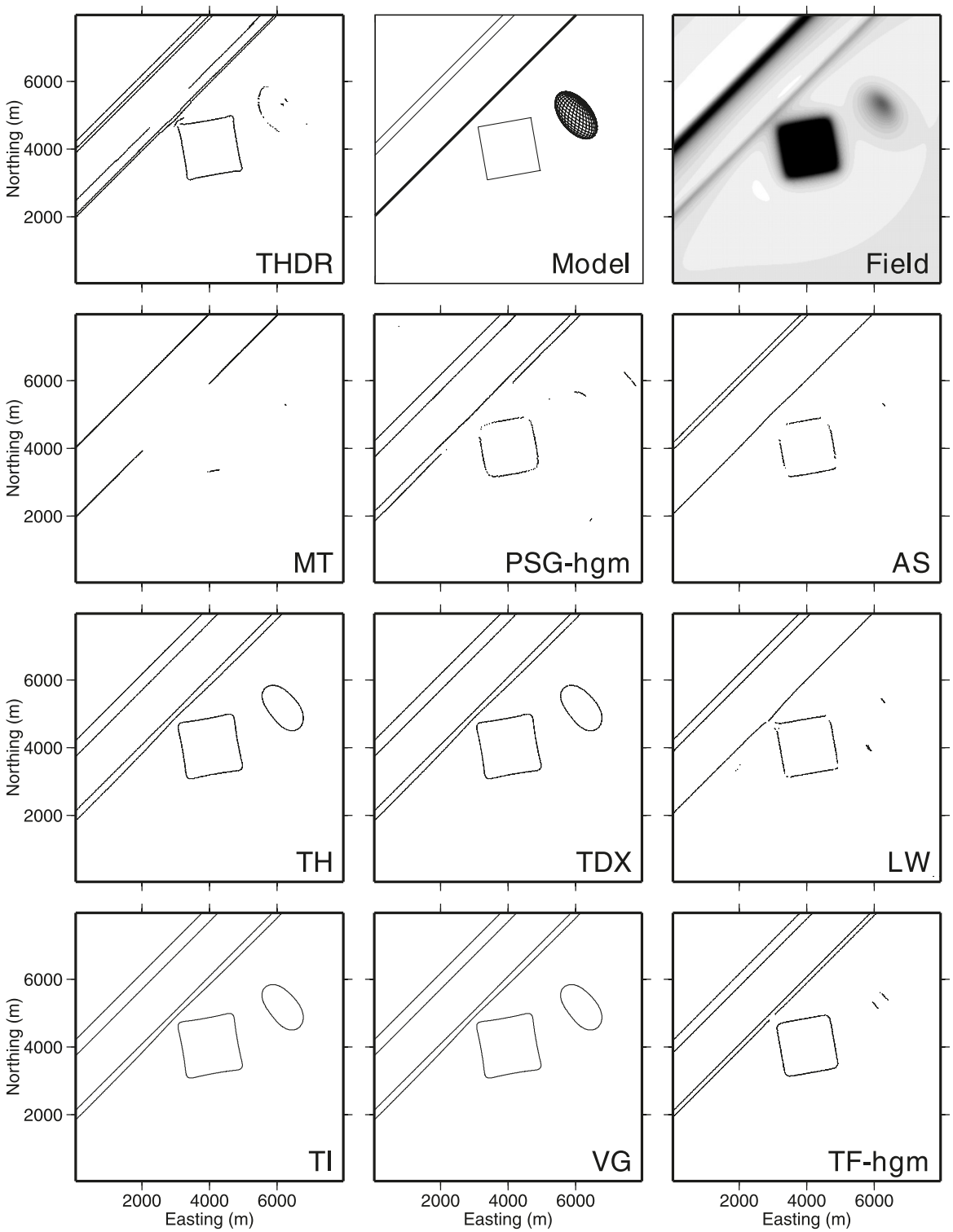

Figure 1. The"model" panel shows the plan view of the synthetic model (see **Table 2** for details), and the "field" panel the synthetic magnetic field produced by the model (data range –18 to +184 nT). Other panels show contact locations calculated from the following enhancements: AS, analytic signal; LW, local wavenumber; MT, magnitude transform; PSG-hgm, pseudogravity horizontal gradient magnitude; TDX, balanced horizontal gradient magnitude; TF-hgm, total field horizontal gradient magnitude; TH, theta; THDR, tilt horizontal gradient magnitude; TI, tilt; VG, vertical gradient.

locate sources, and eight use the position of the maxima of the given enhancement.

All the studied contact mapping techniques are based on two-dimensional (2D) geometries (i.e., appropriate for profile magnetic data). For example, the maxima of the analytic signal and the local wavenumber peak exactly over body edges only for 2D bodies, such as a contact, a sheet, or a body of polygonal cross section. Their application to three-dimensional (3D) bodies, and hence magnetic data in gridded or map form, depends on the degree of curvature of the bodies. For example, the edge of a large batholith can locally be approximated by a contact of large lateral extent. Contact mapping techniques are expected to break down at body corners, but this effect is easy to detect visually.

The synthetic model (**Figure 1**) is made up of four bodies, namely a thin dipping dyke, a thick dipping dyke, a dipping ellipsoid, and a vertical rectangular parallelepiped (see **Table 2** for specific body geometries and physical properties). The geometry of the synthetic bodies was chosen to reflect common geological structures. For example, the edge of the parallelepiped represents a vertical geologic contact between two lithologies having a susceptibility contrast. **Figure 1** shows that all the enhancements map the edges of this body except for the MT, which only exhibits a single maximum at the southern edge of the body. The AS, LW, total field horizontal gradient magnitude (TF-hgm), pseudogravity horizontal gradient magnitude (PSG-hgm), and tilt horizontal gradient magnitude (THDR) functions (**Table 1**) all produce maxima well located over the true edge, and the TI, balanced horizontal gradient magnitude (TDX), theta (TH), and VG functions are displaced slightly outside the body. Theoretically, all the enhancements are expected to perform well because the width to depth ratio of this body is large (= 16). As this ratio decreases, the individual edges become harder to resolve up to the point where the two cannot be mapped separately (for ratios less than unity). Additionally, for small ratios, the estimated contact locations are displaced from the true positions (Pilkington, 2007).

The dipping ellipsoid represents a difficult target for mapping of contacts because it lacks any vertically extensive lateral magnetization contrasts. A contrast exists between the body and its surroundings, but the smoothly varying shape of the ellipsoid causes the resulting magnetic anomaly to be smooth also, and enhancements that determine edge locations based on maxima perform poorly. There are hints of the ellipsoid edge in the AS, LW, TF-hgm, PSG-hgm, and MT maps (**Figure 1**), but all of them have such little continuity or indication of the true body shape that they are practically useless. THDR, on the other hand, responds well enough to suggest the presence of a separate entity and partially maps the ellipsoidal shape. The TI, TDX, TH, and VG enhancements all perform well in delineating a shape indicative of the body, although it is displaced up dip where the maximum of the anomaly is located. These four latter methods respond to the change from negative to positive magnetic field values over the body.

For the thin dyke, i.e., a dyke with a thickness much smaller than the depth to its top, LW, AS, and MT all give a single maximum coincident with the dyke location. THDR is a special case again: it produces a set of three maxima trends, one coincident with the true location but two parallel false trends caused by the dipolar nature of the source (Pilkington and Keating, 2004). All other enhancements erroneously map two edges, with TF-hgm having the smallest separation between them and PSG-hgm, TI, TDX, TH, and VG giving an equally larger apparent dyke width. These latter six methods always produce two apparent contact locations because the magnetic field on either side of the dyke will change from negative to positive and will exhibit an inflection point, equivalent to a maximum in the horizontal gradient. They are also all adversely affected by the dip of the dyke: the calculated contact locations are shifted southwards down dip (Grauch and Cordell, 1987).

For the thick dyke, i.e., a dyke with a width greater than its depth, only MT gives a single maximum, since the deflection of the maximum location towards the body interior is greatest for this enhancement, and the two (expected) maxima merge into one (Pilkington, 2007). All other enhancements are able to resolve the two edges of the dyke. LW does the best job, with nearly perfect locations on both sides, followed by AS, with both maxima displaced slightly inwards towards the dyke centre. In theory, LW and AS should peak at exactly the same location, since LW is the scaled vertical derivative of AS (Pilkington and Keating, 2006). However, the accuracy of the peak location cannot be expected to be any better than the grid interval. TF-hgm gives maxima outside the dyke edges and displaced down dip. PSG-hgm, TI, TDX, TH, and VG map edges farther away from the true sides that are also shifted down dip. THDR accurately maps both edges of the dyke with no dip effects, but again the maxima are accompanied by one other parallel false maxima trend. Sometimes these extra trends can be rejected on the basis of their small amplitudes, but this is not always possible. False maxima trends in THDR may have amplitudes comparable to those of true trends, especially when sources are in close proximity (Pilkington and Keating, 2004).

Table 2. Synthetic model details.

Source[a]	Dip	Depth to top (m)	Width (m)	Depth extent (m)	Susceptibility, SI
Thin dyke	60°SE	100	10	1600	0.05
Thick dyke	60°SE	100	250	1600	0.01
Ellipsoid	60°SW	220	1600, 400	1800	0.02
Rectangular parallelepiped	90°	100	1600	5000	0.01

[a]All induced in a vertical field of 50 000 nT.

The results of **Figure 1** show that no single enhancement is capable of providing accurate contact or edge locations for all types of magnetic sources. From theory, MT, AS, LW, and THDR should map isolated contacts perfectly, even if they are dipping or remanent magnetization is present (see references in **Table 1**). In contrast, locations calculated from the remaining enhancements are compromised by both of these conditions. All techniques will suffer from interference effects, i.e., when sources are close enough that their anomalies overlap, since the combined anomaly shape will differ from the theoretical response used in synthetic calculations. The kinds of effects from interference can be seen in **Figure 1** where the parallelepiped comes close to the thin dyke, leading to a loss (MT, PSG-hgm), or deflection of solutions (LW) or presence of false trends (THDR). Overall, the TI, TDX, TH, and VG maps show the best continuity; however, these four have the greatest sensitivity to nonvertical dips. As Pilkington and Keating (2004) point out, using more than one approach is always recommended since co-located solutions from different methods provide increased confidence in the reliability of a given contact location and lessen the adverse effects of source magnetization direction and nonvertical geological dip. The issue of noise on the performance of each of the enhancements has not been addressed but is dealt with in the following section dealing with real data where the qualitative part of predictive geologic mapping is discussed.

Chibougamau data

Figure 2 shows the magnetic field and the mapped geology of a portion of the Abitibi Greenstone Belt near Chibougamau, Quebec. The magnetic field map clearly shows the predominant east–west-striking geologic trends in this region, with the more magnetic units (stronger magnetic field) occurring in the south. Some broad correlations can be made. The highest amplitude magnetic features on the map are caused by peridotitic rocks of the Roberge Formation. Smaller amplitude highs are associated with ferrogabbros occurring within anorthosite of the Lac Doré Formation in the southeast. Magnetic lows or subdued zones are generally associated with the felsic Blondeau and Waconichi formations. On the other hand, some mafic lithologies do not show a significant magnetic effect, e.g., the Bourbeau and Ventures rocks. Often, more mafic lithologies have more Ti-rich magnetites, which results in lower susceptibilities. Many magnetic trends can be seen within the Gilman Formation (volcanics), suggesting a possible subdivision into mafic and felsic flows.

Figure 3 shows mapped contacts using the same procedures as those used for the synthetic example in **Figure 1**. The relative performance of the enhancements is much different now that real data containing the combined effects of tie-line levelling, gridding, and other corrections are used. The most strongly affected are AS and LW, which show poor continuity along geologic strike. This effect is predominantly due to gridding, which leads to well-defined maxima in both the AS and LW functions at locations where a flightline crosses a magnetization boundary but a lack of maxima at gridded locations between the flightlines. Hence, the mapped contact locations are concentrated along each flightline, and this is most clear in the case of the LW, where the breakup of trends, particularly those with short lengths, limits its mapping capability. This effect can be partially overcome by an upward continuation of the field, but this would be at the cost of reduced spatial resolution. The remaining enhancements can be divided into groups, each having similar results in terms of the number and location of mapped contacts. PSG-hgm and MT are similar in having a smaller number of solutions but with much better continuity than AS and LW. The former two enhancements result in functions with a level of smoothness or complexity similar to that of the observed magnetic field (Cordell and Grauch, 1985; Stavrev and Gerovska, 2000). No derivatives are involved in their calculation, so they have a high level of stability in the presence of noise, gridding effects, etc.

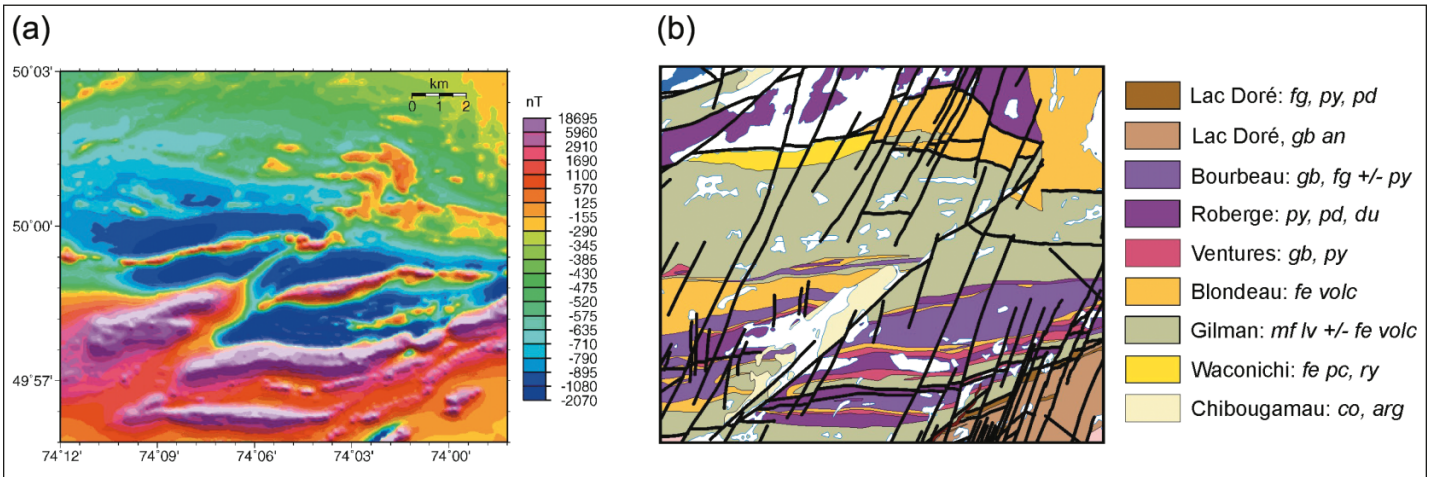

Figure 2. (a) Magnetic field over portion of Chibougamau area, Abitibi Greenstone Belt, Quebec, Canada. (b) Geological map of the area in (a). arg, argillite; co, conglomerate; du, dunite; fe pc, felsic pyroclastics; fe volc, felsic volcaniclastics; fg, ferrogabbro; gb, gabbro; gb an, gabbroic anorthosite; mf lv, mafic lavas; pd, peridotite; py, pyroxenite; ry, rhyolite. Solid black lines denote faults.

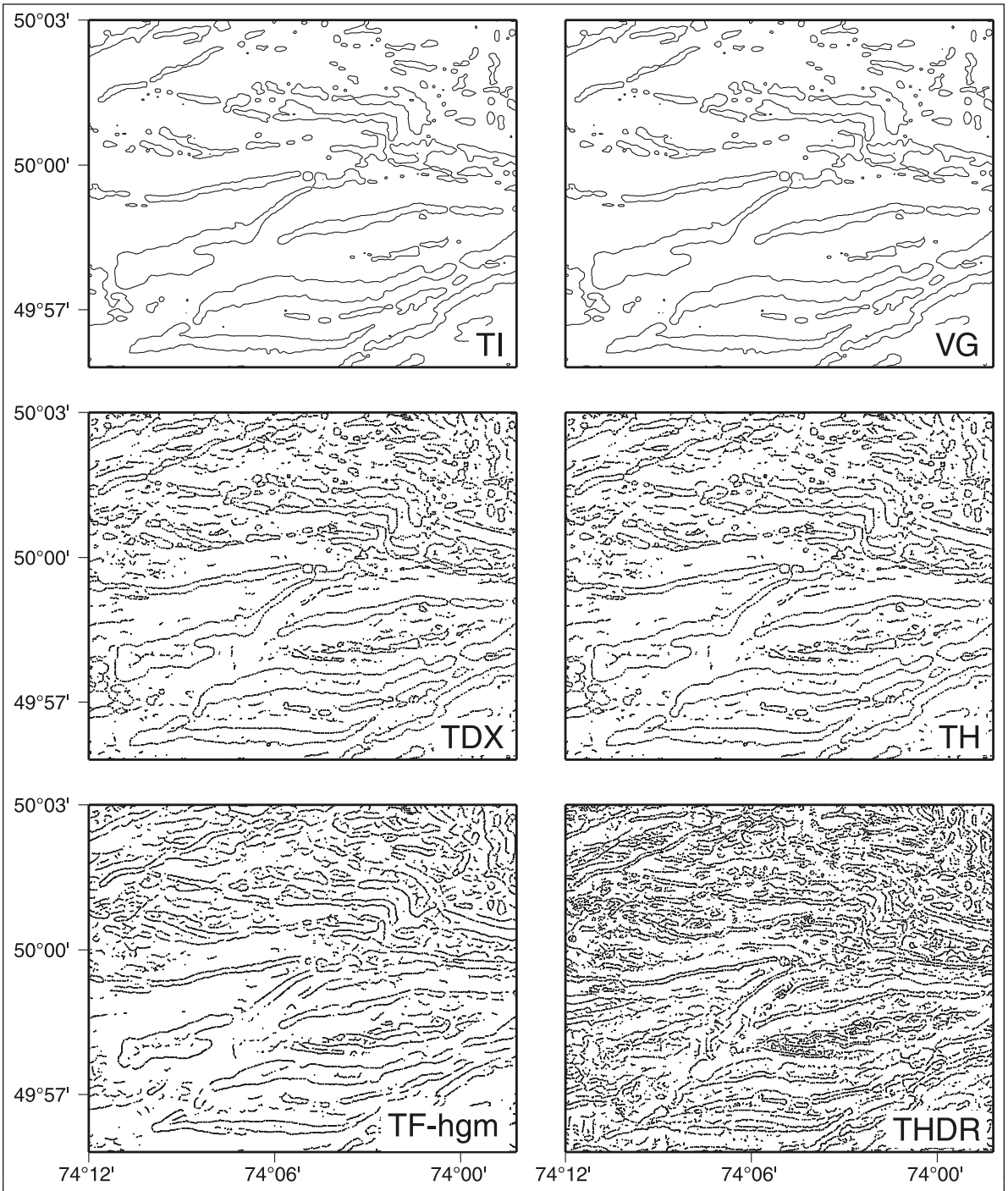

Figure 3. Contact locations for the Chibougamau area calculated from the following enhancements: AS, analytic signal; LW, local wavenumber; MT, magnitude transform; PSG-hgm, pseudogravity horizontal gradient magnitude; TDX, balanced horizontal gradient magnitude; TF-hgm, total field horizontal gradient magnitude; TH, theta; THDR, tilt horizontal gradient magnitude; TI, tilt; VG, vertical gradient.

In contrast, the LW transform involves second-order derivatives, which explains its less stable performance.

The TI and VG maps are actually equivalent, as are the TDX and TH maps. All contact locations present in the TI and VG maps are also contained in the TDX and TH maps, hence the high degree of similarity between the two groups (**Figure 3**). For the synthetic data, these four enhancements give exactly the same solutions. Inspection of the formula for these enhancements (**Table 1**) shows that the zero values of VG and TI are equivalent, since if, and only if, the VG (df/dz) is zero, then the TI ($\tan^{-1}\{(df/dz)/[(df/dx)^2 + (df/dy)^2]^{1/2}\}$) will also be zero. Considering the TDX and TH results, we note that Wijns et al. (2005) actually defined the mapped quantity TH (**Table 2**) as cos θ, where θ is the tilt angle given by TI (Li, 2006).

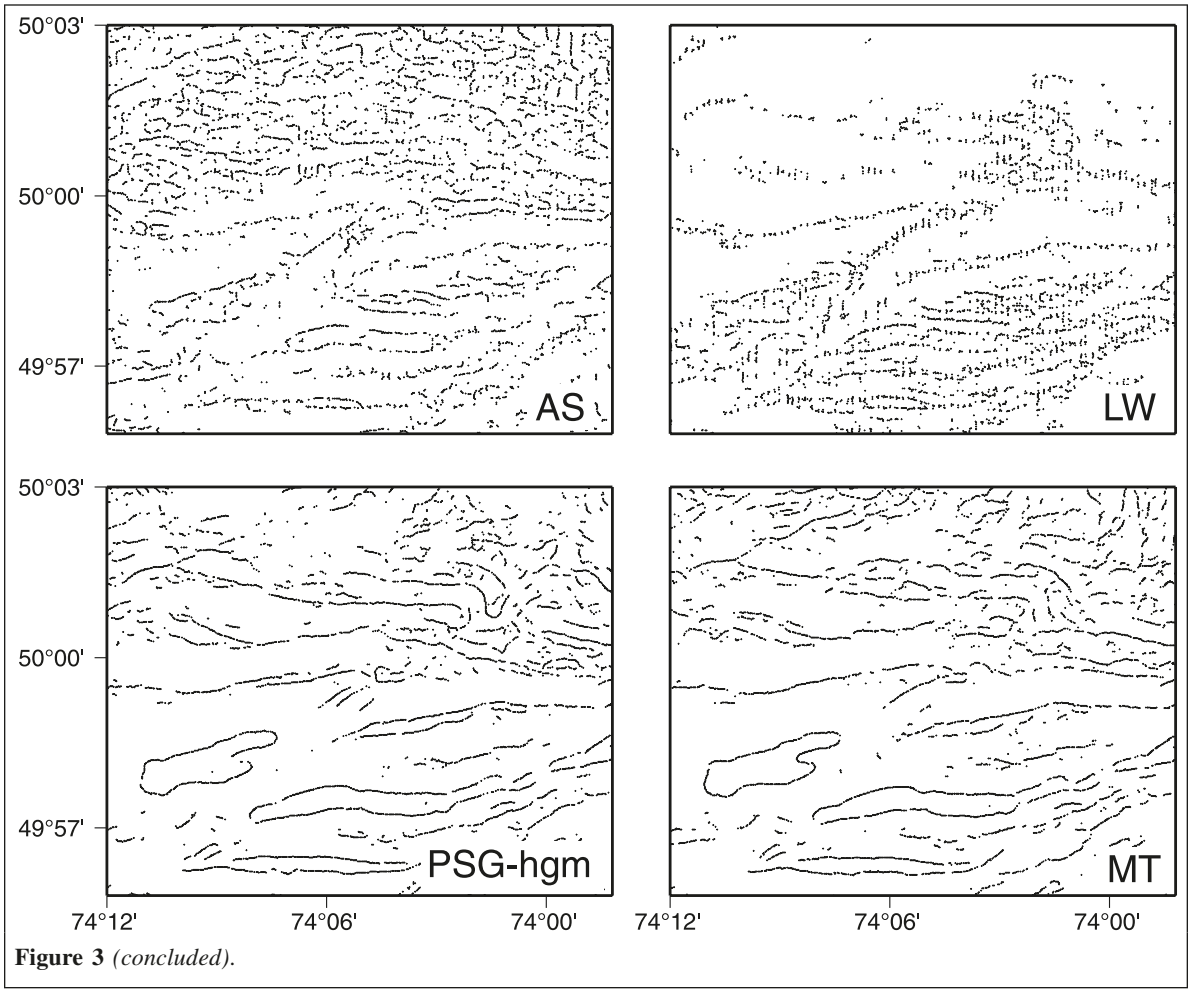

Figure 3 *(concluded).*

Therefore, TH varies from 0 to 1 and TI varies from –90° to +90°, and a maximum in TH corresponds to a zero value for TI. From the expression for TDX, it follows that sin(TDX) = cos θ, with TDX ranging from 0° to 90°. Consequently, maxima from the TDX enhancement are equivalent to those in TH, and both of these are equivalent to a zero value of TI (θ) and VG. This equivalence is made clear in the synthetic example. There are more maxima (TDX, TH) than zero values (TI, VG) in the real data example because of interference between anomalies. A nearby source may raise or lower the level of another anomaly, so the amplitude of the latter is either always above or below the zero level, but a maximum is still calculated by the TDX and TH expressions. Thus, in terms of contact locations we can replace all four enhancements with just one (either TDX or TH).

TF-hgm produces a distribution of contacts similar to that of the previous four enhancements. Although theoretically it is susceptible to false maxima trends, in practice this seems to be limited to strongly dipolar sources, e.g., thin shallowly dipping dykes (Grauch et al., 2001). Thus, for steeply dipping Precambrian Shield regions, most maxima will correspond to real contacts. The last set of results is given by the THDR function, which, similar to its behaviour in the synthetic model, leads to the greatest number of solutions. Many of these contact locations are false trends that parallel the real contacts and are caused by interference from adjacent anomalies. These false trends can be identified often when the contacts are overlain on the magnetic field map: the true contacts will always be associated with the flanks of a given anomaly.

In addition to locating contacts, which constitutes the quantitative part of predictive mapping, potential field enhancements form the basis for the qualitative part: dividing an area into subregions with similar geophysical characteristics. **Figure 4** shows the subset of enhancements (VG, TI, DR, and directional tilt (Ty)) from **Table 1** that can be used in this fashion applied to the Chibougamau data. The remaining enhancements are not considered, since they are only applicable to locating contacts: these functions exhibit maxima over magnetization contrasts and lead to a more complicated image to interpret compared to those shown in **Figure 4**. Predictive mapping based on visual classification of maps benefits from the improved correlation between geology and magnetic anomalies that can result from applying particular enhancements.

The vertical gradient (VG) enhancement is essentially a high-pass filter, suppressing long-wavelength anomalies caused by large-scale or deep structures and emphasizing the shorter wavelength anomalies associated with near-surface sources, i.e., the outcropping geology to be classified. The

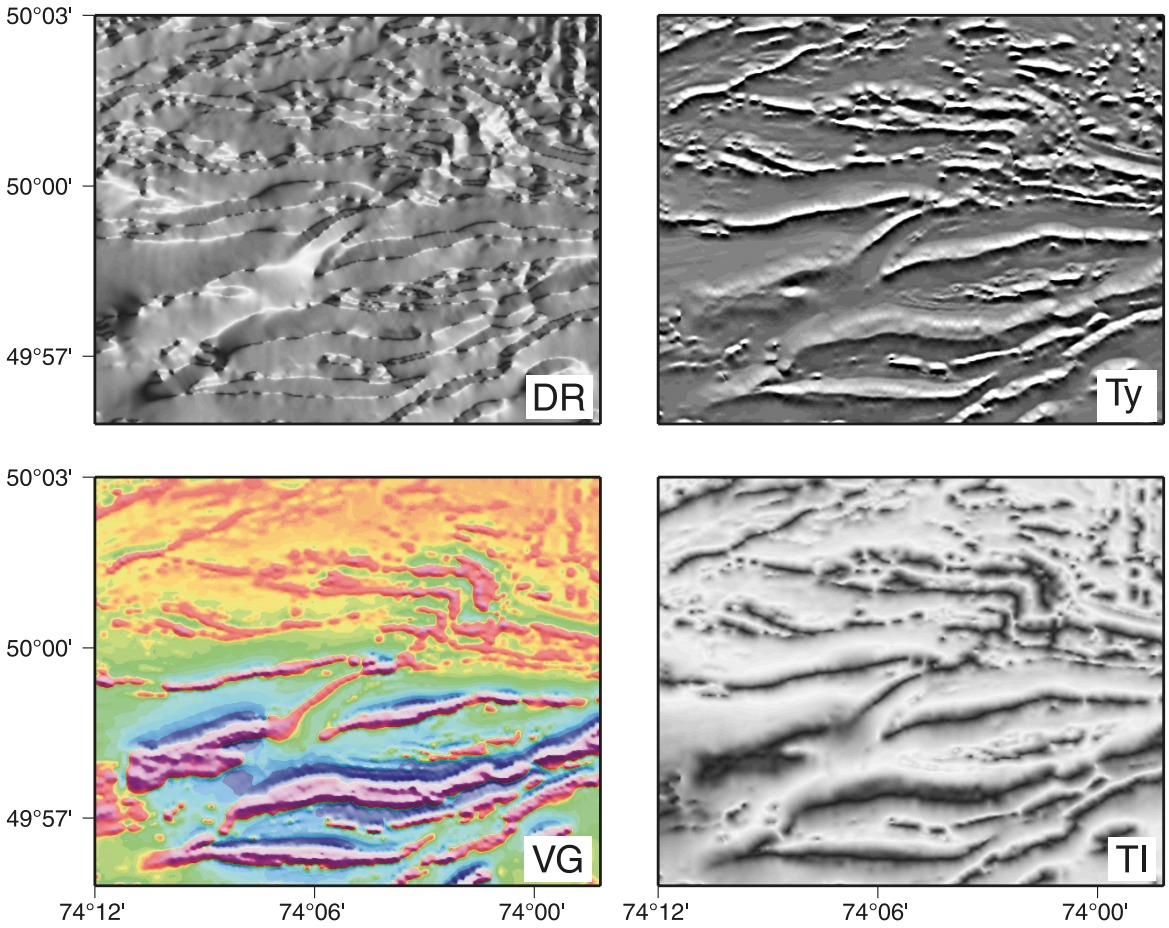

Figure 4. Images of the following enhancements for the Chibougamau area: DR, derivative ratio (range –90° to +90°); TI, tilt (range –90° to +90°); Ty, directional tilt (range –90° to +90°); VG, vertical gradient (range –16 to +23 nT/m).

high-amplitude east–west-trending anomalies in the southern part of the map are now better resolved by the VG (**Figure 4**); the anomaly widths have decreased, and in some cases a single magnetic field anomaly in the magnetic field (**Figure 2a**) is now resolved into two separate gradient anomalies (e.g., at 49°58′N, 74°09′W). Hence, the VG map sharpens up the definition of features in the magnetic field, with this increased detail enabling an improved classification of geologic units. Note that the broad change from high- to low-amplitude anomalies going northwards is preserved in the VG map. This is not the case for the other three quantities in **Figure 4**, namely TI, DR, and Ty. As its name implies, the directional tilt Ty enhances features having a certain strike. Since the dominant strike in the Chibougamau region is east–west, the Ty was used to emphasize features in the *x* direction. Cooper and Cowan (2006) point out that the chosen azimuth for the directional tilt is not limited to the *x* and *y* directions. The TI, DR, and Ty enhancements all involve taking ratios of certain magnetic field derivatives (**Table 1**), which leads to a loss of amplitude information, but a balancing of responses between areas with different amplitudes. The prominence of high-amplitude anomalies (in the south) versus low-amplitude (in the north) anomalies is therefore reduced, and all anomalies now have similar expressions in the TI, DR, and Ty maps. This balancing effect is useful in regions where field values have a large dynamic range and images of the magnetic field or the VG are dominated by only the highest amplitude features. Structures and magnetization contrasts causing relatively weak anomalies are then emphasized by the TI, DR, and Ty enhancements.

Calculating the DR leads to a stepped-slope appearance (**Figure 4**) with the maximum change in value occurring over the centres of magnetized sources. Edges of bodies are not well defined, and the DR values show limited variation in between sources. Therefore, the DR enhancement does not appear to offer any advantages over existing products such as the TI and VG methods. The directional tilt Ty essentially acts like a horizontal derivative filter coupled with a balancing of amplitudes so that anomaly magnitude has a minimal effect. This is clear in **Figure 4**, where Ty values in the northern part of the area have amplitudes and character comparable to those in the south. The information content of the Ty map is very similar to that of the TI map, the only difference being a phase shift between the two maps such that positively magnetized sources are associated with only positive TI values but produce coupled

high–low combinations in the Ty map. This added complication does not appear to provide any significant advantages over the features mapped in the TI image.

Higher order variants

Several variants of the enhancements discussed previously have been introduced to improve the resolution or definition of features in the magnetic field. These mostly involve replacing first derivatives (**Table 1**) with second- or variable-order versions, e.g., second-order TI (Cooper and Cowan, 2006), second-order AS (Debeglia and Corpell, 1997), second-order LW (Smith et al., 1998), variable-order VG (Cooper and Cowan, 2004), and variable-order TF-hgm (Fedi and Florio, 2001). The effects of higher order derivatives are generally similar, leading to a theoretically better resolution of short-wavelength anomalies and greater suppression of deeper source effects, but in practice resulting in an attendant increase in the obscuring effects of noise. The adverse effects of higher order derivatives are usually concentrated along flightlines, leading to unwanted linear features parallel to the survey line direction. Consequently, using second-order derivatives is usually recommended only in the case of recent, high-quality, global positioning system (GPS) located surveys. Over sedimentary or mixed sedimentary–crystalline areas where anomalies may be weak, i.e., <5 nT, the second vertical derivative will enhance these small anomalies. On the other hand, in areas of exceptionally strong and overlapping magnetic anomalies, such as in the Chibougamau example, it provides a means to resolve closely spaced features. Of all the enhancements in **Table 2**, only LW uses derivatives of order greater than one, with the adverse effects being clear in **Figure 3**.

Beyond enhancements

Our discussion of quantitative methods of predictive mapping has been limited to mapping contact locations or, equivalently, lateral magnetization contrasts. This is not the only possible application of potential field data to the mapping problem. Gravity and magnetic data and their enhancements can also be used in classification/modelling algorithms that attempt to automate the visual pattern recognition approach usually done manually by an interpreter. However, Parsons et al. (2006) show the difficulties in this approach by finding that statistical analyses based on amplitudes result in no simple or direct correlation between mapped geology and observed magnetic field. The statistical approach may work well in one area but fail in an adjacent area, thus precluding its use as a reliable predictive mapper. Holden et al. (2008) treat a slightly different problem and evaluate the prospectivity of an area for gold deposits based on the magnetic expressions of geologic discontinuities and areas of complex structure/lithology. The most prospective areas are those where discontinuities and geological complexity are close. The success of the Holden et al. approach (they find 76% of known deposits) is probably due to avoiding any type of lithological classification and just focusing on structural and textural signatures in the magnetic data.

As classification and modelling algorithms become more effective, there will however always be a need for a manual component in the mapping process, particularly at the revision stage, where the match between geophysical information and mapped geology is checked and possibly updated.

Conclusions

A wide range of potential field enhancements are available to assist in geologic mapping. Many have been introduced recently, with nine out of the 12 listed in **Table 1** postdating 1993. Regarding the question posed in the Introduction (Are some enhancements redundant, useless, confusing?), the answer is yes, in some cases. Several enhancements were seen to be redundant for contact mapping, with the tilt (TI), vertical gradient (VG), balanced horizontal gradient magnitude (TDX), and theta (TH) methods providing almost identical solutions. Either the TDX or TH maps can be used in place of all four techniques. The theoretical expressions for these quantities show that this is a true redundancy. In the case of pseudogravity horizontal gradient magnitude (PSG-hgm) and magnitude transform (MT), we note that the similarity of the mapped contacts can be considered a practical redundancy, so both maps are not needed. Since the operations involved in calculating PSG-hgm are more often used in magnetic data processing, this is the more practical choice of the two. None of the enhancements appeared useless, but the analytic signal (AS) and local wavenumber (LW) methods were susceptible to flightline effects, leading to break down of the continuity of mapped contacts. As far as confusing, only the tilt horizontal gradient magnitude (THDR) falls in this class, since the presence of extra, false contact locations can complicate mapping, especially in areas of complex source distributions. Concerning the use of enhancements to derive images for qualitative mapping, only four of the listed 12 are possibly useful. However, two of these, the derivative ratio (DR) and directional tilt (Ty), appear to offer little advantage over the TI and VG images, which have a similar level of detail but differ in the treatment of amplitude information.

Table 1 summarizes the question of how these enhancements are related to the physical property of interest, i.e., source magnetization. Of the 12 listed, eight exhibit maxima and two reach a value of zero over a contact. The two others have no simple, direct relationship that is easily used. Therefore, most of these enhancements have a physical meaning that can be exploited in interpretation. How well this relationship fares in the presence of noise, nonvertical dips, and nonvertical magnetizations ultimately determines their practical utility.

Acknowledgments

This work has been done as part of the Remote Predictive Mapping Project, a component of the Geoscience for Energy and Minerals Program of Natural Resources Canada. Warner Miles and three anonymous reviewers provided helpful

comments. This is Geological Survey of Canada Contribution 20090029.

References

Barnes, A.E. 2007. Redundant and useless seismic attributes. *Geophysics*, Vol. 72, pp. 33–38.

Blakely, R.J., and Simpson, R.W. 1986. Approximating edges of source bodies from magnetic or gravity anomalies. *Geophysics*, Vol. 51, pp. 1494–1498.

Boyd, D. 1967. The contribution of airborne magnetic surveys to geological mapping. In *Mining and groundwater geophysics/1967*. Edited by L.W. Morley. Economic Geology Report 26, Department of Energy, Mines and Resources, Ottawa, Ont. pp. 213–227.

Chopra, S., and Marfurt, K.J. 2007. *Seismic attributes for prospect identification and reservoir characterization*. Society of Exploration Geophysicists, Tulsa, Okla.

Cooper, G.R.J., and Cowan, D.R. 2004. Filtering using variable order vertical derivatives. *Computers & Geosciences*, Vol. 30, pp. 455–459.

Cooper, G.R.J., and Cowan, D.R. 2006. Enhancing potential field data using filters based on the local phase. *Computers & Geosciences*, Vol. 32, pp. 1585–1591.

Cooper, G.R.J., and Cowan, D.R. 2007. Enhancing linear features in image data using horizontal orthogonal gradient ratios. *Computers & Geosciences*, Vol. 33, pp. 981–984.

Cordell, L.E., and Grauch, V.J.S. 1985. Mapping basement magnetization zones from aeromagnetic data in the San Juan Basin, New Mexico. In *The utility of regional gravity and magnetic anomaly maps*. Edited by W.J. Hinze. Society of Exploration Geophysicists, Tulsa, Okla. pp. 181–197.

Debeglia, N., and Corpel, J. 1997. Automatic 3-D interpretation of potential field data using analytic signal derivatives. *Geophysics*, Vol. 62, pp. 87–96.

Fedi, M., and Florio, G. 2001. Detection of potential fields source boundaries by enhanced horizontal derivative method. *Geophysical Prospecting*, Vol. 49, pp. 40–58.

Gay, S.P., and Hawley, B.W. 1991. Syngenetic magnetic anomaly sources: Three examples. *Geophysics*, Vol. 56, pp. 902–913.

Grauch, V.J.S., and Cordell, L. 1987. Limitations of determining density or magnetic boundaries from the horizontal gradient of gravity or pseudogravity data. *Geophysics*, Vol. 52, pp. 118–121.

Grauch, V.J.S., Hudson, M.N., and Minor, S.A. 2001. Aeromagnetic expression of faults that offset basin fill, Albuquerque basin, New Mexico. *Geophysics*, Vol. 66, pp. 707–720.

Hart, B.J. 2008. Stratigraphically significant attributes. *The Leading Edge*, Vol. 27, No. 3, pp. 320–324.

Holden, E.-J., Dentith, M., and Kovesi, P. 2008. Towards the automated analysis of regional aeromagnetic data to identify regions prospective for gold deposits. *Computers & Geosciences*, Vol. 34, pp. 1505–1513.

Hood, P.J. 1965. Gradient measurements in aeromagnetic surveying. *Geophysics*, Vol. 30, pp. 891–902.

Isles, D.J., Harman, P.G., and Cunneen, J.P. 1989. The contribution of high resolution aeromagnetics to Archean gold exploration in the Kalgoorlie region, Western Australia. In *The geology of gold deposits*. Edited by R.R. Keays, W.R.H. Ramsay, and D.I. Groves. Economic Geology Monograph 6, pp. 389–397.

Jacques, A.L., Wellman, P., Whitaker, A., and Wyborn, D. 1997. High-resolution geophysics in modern geological mapping. *AGSO Journal of Australian Geology & Geophysics*, Vol. 17, pp. 159–174.

Li, X. 2006. On "Theta map: Edge detection in magnetic data" (C. Wijns, C. Perez, and P. Kowalczyk, Geophysics, 70, L39–L43). *Geophysics*, Vol. 71, p. X11.

Li, X. 2008. Seismic attributes and gravity and magnetic transformations: The same mathematics under different names for different geophysical data sets. In *Proceedings of the 78th Annual International Meeting of the Society of Exploration Geophysicists*, 9–14 November 2008, Las Vegas, Nev. Society of Exploration Geophysicists, Tulsa, Okla., Expanded Abstracts, Vol. 27, pp. 839–843.

Miller, H.G., and Singh, V. 1994. Potential field tilt — a new concept for location of potential field sources. *Journal of Applied Geophysics*, Vol. 32, pp. 213–217.

Milligan, P.R., and Gunn, P.J. 1997. Enhancement and presentation of airborne geophysical data. *AGSO Journal of Australian Geology & Geophysics*, Vol. 17, pp. 63–76.

Parsons, S., Nadeau, L., Keating, P., and Chung, C.-J. 2006. Optimizing the use of aeromagnetic data for predictive geological interpretation: an example from the Grenville Province, Quebec. *Computers & Geosciences*, Vol. 32, pp. 565–576.

Pilkington, M. 2007. Locating geologic contacts with magnitude transforms of magnetic data. *Journal of Applied Geophysics*, Vol. 63, pp. 80–89.

Pilkington, M., and Keating, P. 2004. Contact mapping from gridded magnetic data — a comparison of techniques. *Exploration Geophysics*, Vol. 35, pp. 306–311.

Pilkington, M., and Keating, P. 2006. The relationship between local wavenumber and analytic signal in magnetic interpretation. *Geophysics*, Vol. 70, pp. L1–L3.

Roest, W.R., Verhoef, J., and Pilkington, M. 1992. Magnetic interpretation using the 3-D analytic signal. *Geophysics*, Vol. 57, pp. 116–125.

Roy, A., and Aina, A.O. 1986. Some new magnetic transformations. *Geophysical Prospecting*, Vol. 34, pp. 1219–1232.

Smith, R.S., Thurston, J.B., Dai, T.F., and MacLeod, I.N. 1998. iSPI — the improved source parameter imaging method. *Geophysical Prospecting*, Vol. 46, pp. 141–151.

Stavrev, P., and Gerovska, D. 2000. Magnetic field transforms with low sensitivity to the direction of source magnetization and high centricity. *Geophysical Prospecting*, Vol. 48, pp. 317–340.

Thurston, J.B., and Smith, R.S. 1997. Automatic conversion of magnetic data to depth, dip, and susceptibility contrast using the SPI method. *Geophysics*, Vol. 62, pp. 807–813.

Verduzco, B., Fairhead, J.D., Green, C.M., and MacKenzie, C. 2004. New insights into magnetic derivatives for structural mapping. *The Leading Edge*, Vol. 23, No. 2, pp. 116–119.

Wijns, C., Perez, C., and Kowalczyk, P. 2005. Theta map: Edge detection in magnetic data. *Geophysics*, Vol. 70, pp. L39–L43.

